

## Polydispersity Exponent in Homogeneous Droplet Growth

J. A. Blackman<sup>1</sup> and S. Brochard<sup>2</sup>

<sup>1</sup>*Department of Physics, University of Reading, Whiteknights, Reading RG6 6AF, United Kingdom*

<sup>2</sup>*Laboratoire de Métallurgie Physique, Unité Mixte de Recherche 6630 du CNRS, Université de Poitiers, BP 179, 86962 Futuroscope Chasseneuil Cedex, France*

(Received 27 December 1999)

The homogeneous growth of  $D$ -dimensional hyperspherical droplets on a  $d$ -dimensional surface produces a bimodal distribution in the sizes of the droplets, with a roughly monodispersed distribution of larger droplets superimposed on a highly polydisperse distribution of smaller ones. The polydisperse regime is characterized by an exponent, which also determines the total droplet density. The exponent is evaluated, and it is deduced that  $d = 3$  represents an upper critical dimensionality.

PACS numbers: 81.15.Aa, 02.50.-r, 68.55.-a

The condensation of droplets on a surface and their subsequent coalescence and growth is a basic process in a large class of phenomena in both nature and materials science [1]. The characteristic pattern of droplets that evolves when water condenses on a cold surface (breath figures) has been well studied [2–5]. Related patterns are seen in the late stage of vapor deposition of thin films [6–14], surfactant limited aggregation of hydrophobic molecules in water [15], and in flyash formation during pulverized coal combustion [16].

A decade ago, Family and Meakin [7,8] introduced a model that contained the essentials of droplet growth. The model consists of hyperspherical droplets with dimensionality  $D$ . When a droplet of radius  $r_1$  overlaps a droplet of radius  $r_2$ , a new droplet is formed with radius  $r$  given by  $r = (r_1^D + r_2^D)^{1/D}$ . Two models were proposed for coalescence and growth on a  $d$ -dimensional surface. In the *heterogeneous* model, there are a fixed number of defect sites on the substrate, and growth occurs by condensation of vapor at these sites, with coalescence taking place when neighboring droplets overlap. For *homogeneous* nucleation, new elementary droplets of radius  $r_0$  are introduced randomly onto the surface at a constant rate. There is no mobility in the model, and so the focus is entirely on the process of growth through coalescence.

Scaling behavior is observed in these systems, and there have been a number of theoretical treatments [7,8,17–26]. With heterogeneous nucleation, the particle size distribution displays a single peak, and this case is rather well understood. In contrast, the homogeneous model exhibits a bimodal size distribution, but the theoretical understanding is as yet incomplete. Bimodal distributions have been observed in a number of experimental situations [5,6,10,12,14,15]. This paper addresses the homogeneous model. The bimodal distribution comprises a roughly monodispersed distribution of larger droplets superimposed on a highly polydispersed distribution of smaller droplets. The behavior of the growth is a delicate balance between the larger and the smaller droplets. The larger droplets determine a characteristic length scale for the

process, while the total droplet density is determined by the much larger number of polydisperse smaller droplets.

The polydispersity is expressed in terms of an exponent  $\tau$ , such that the number of islands of size  $s$  is given by  $N_s \sim s^{-\tau}$ . Currently numerical values of  $\tau$  are estimated by computer simulations, but to our knowledge no analytic expressions are available. The object of the present work is to provide for the first time an analytic evaluation of this exponent.

We begin by summarizing what is known about the scaling properties of the model. The size distribution for droplets of size  $s$  at time  $t$  can be written in the usual scaling form

$$N_s(t) \sim s^{-\theta} f(s/S(t)), \quad (1)$$

where  $S(t)$  is the mean cluster size. The bimodal distribution is expressed explicitly by writing the scaling function as

$$f(x) = x^{\theta-\tau} g(x) + h(x), \quad (2)$$

where  $h(x)$  represents the large droplet peak, and the other term describes the smaller droplets, with  $g(x)$  varying slowly with  $x$ . It is useful to define moments of the distribution function

$$M_n = \sum_s s^n N_s(t), \quad (3)$$

where  $n$  is an arbitrary real number. Two more exponents  $z$  and  $z'$  are introduced to describe the time evolution of the mean cluster size  $S(t)$  and the cluster density  $N(t)$ ,

$$S(t) = M_2/M_1 \sim t^z, \quad (4)$$

$$N(t) = M_0 \sim t^{-z'}. \quad (5)$$

The moments can be evaluated from Eqs. (1)–(3). For small values of  $n$ , the lower limit of the summation dominates and this leads to the result

$$\begin{aligned} M_n &\sim t^{z(n-\theta+1)} && \text{if } n \geq \tau - 1, \\ &\sim t^{z(\tau-\theta)} && \text{if } n \leq \tau - 1. \end{aligned} \quad (6)$$

The constant deposition rate, implying that  $M_1 \sim t$  gives the standard result  $z(2 - \theta) = 1$ . The fractional coverage  $C$  is proportional to  $M_{d/D}$  for  $D$ -dimensional hyperspheres on a  $d$ -dimensional surface. Now  $C$  approaches 1 in the asymptotic time limit provided  $D > d$ . If  $D = d$  complete coverage occurs after a finite elapse of time. From Eq. (6),  $M_{d/D}$  approaches a constant value if

$$\theta = 1 + d/D \quad (7)$$

with the requirement that  $d/D \geq \tau - 1$ , or  $\tau \leq \theta$ . Hence

$$z = D/(D - d). \quad (8)$$

For all cases [8],  $\tau \geq 1$ , and so

$$z' = z(\theta - \tau). \quad (9)$$

An important feature that will emerge is that the key rate determining quantities scale with the cluster density  $N$ . The first is the fractional coverage  $C$  for which we can write  $(1 - C) \sim N$ . This is illustrated in Fig. 1, which shows results from simulations for the  $d = 2, D = 3$  case. We can understand the scaling with  $N$  as follows. In the simplest case ( $d = 1$ ), the number of gaps between droplets is equal to the number of droplets,  $N$ , while the mean gap size can be shown to remain constant throughout the scaling regime. This invariance stems from the fact that the length scale determining the distribution of gap sizes is the fixed quantity  $2r_0$ . The fraction of uncovered surface,  $(1 - C)$ , varies as  $N$ , therefore. At low surface coverage, there is a single length scale in the problem, namely,  $S(t)$  while, in the coalescence regime, there are *two* characteristic lengths,  $S(t)$  and  $2r_0$ . The above argument can be extended to arbitrary surface dimensionality. For example, for  $d = 2$ , the droplets are closely packed with a separation determined by  $2r_0$ . The free surface area will scale, therefore, as the mean circumference of the droplets on the surface. Generalizing to arbitrary  $d$  and  $D$ , the free surface area scales like  $M_{(d-1)/D}$ , which in turn scales like

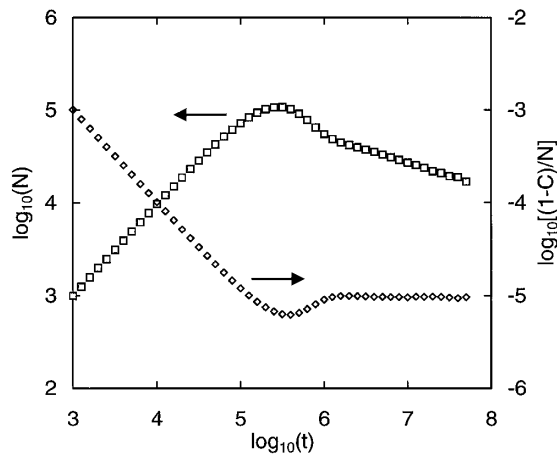


FIG. 1. Simulations of  $D = 3$  droplet growth on  $d = 2$  square surface of side  $1400r_0$  with periodic boundary conditions.  $N$  and  $(1 - C)/N$  are shown as functions of time (number of Monte Carlo steps).

$N$  if  $1 + (d - 1)/D \leq \tau$ . The values of  $\tau$  that we shall derive satisfy this condition.

Scaling behavior in these systems occurs at fairly high coverages, and we need to consider which are the dominant processes in this regime. When a new droplet is added, the following possibilities occur:

(1) The droplet falls on the free surface without touching an existing droplet.

(2) The new droplet falls on an existing one whose radius increases as a result of the coalescence. There are then two possibilities: *either* (a) the expanding droplet does not touch another one, *or* (b) it does touch another resulting in a further coalescence.

(3) The droplet falls so as to bridge two clusters that are close together causing them to coalesce. This process is rare during the early stages of growth, but it plays a major role in this regime.

(4) There are other possible scenarios; both cases 2(b) and 3 could result in further coalescences. It is found from simulations that such cascade processes almost never occur for  $d = 1$ . They do take place for  $d = 2$ , however, and often quite dramatically. We include all cascade processes in category 4.

The number of droplets on the surface increases by 1 in process 1, decreases by 1 in processes 2(b) and 3, and does not change in case 2(a). In the fourth case, there is a decrease in the number, which is 2 or greater. Let us denote the number of droplets that have been created or destroyed by each of the processes up to time  $t$  as  $n_1, n_{2b}, n_3$ , and  $n_4$ , so that the total droplet density  $N$  is given by

$$N = n_1 - n_{2b} - n_3 - n_4. \quad (10)$$

Similarly, the change in surface coverage since the start of the deposition can be tracked separately for each process. There is an increase in cases 1 and 2(a), and a decrease with 2(b), 3, and 4, so that, in an obvious notation

$$C = c_1 + c_{2a} - c_{2b} - c_3 - c_4. \quad (11)$$

The individual contributions to the droplet density and surface coverage were obtained from simulations, and their time derivatives deduced. With subscript  $\alpha$  denoting the process (excluding  $\alpha = 2a$  for the number count), and using a dot over the symbol to indicate a time derivative, we find that all the quantities scale with the droplet density.

$$\dot{n}_\alpha \sim \dot{c}_\alpha \sim N. \quad (12)$$

The results for  $d = 2, D = 3$  are plotted in Figs. 2 and 3, and similar behavior was observed in simulations on  $d = 1, D = 2$  systems. In view of Eqs. (10) and (11), this leads to rate determining conditions

$$\dot{n}_1 - \dot{n}_{2b} - \dot{n}_3 - \dot{n}_4 \sim 0 \quad (13)$$

and

$$\dot{c}_1 + \dot{c}_{2a} - \dot{c}_{2b} - \dot{c}_3 - \dot{c}_4 \sim 0, \quad (14)$$

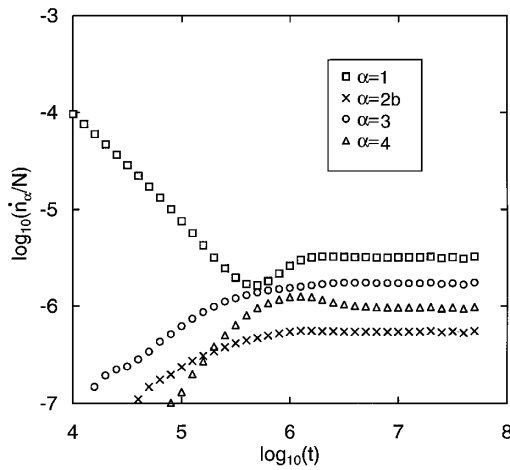


FIG. 2. Plots of  $\dot{n}_\alpha/N$  against time for same system as Fig. 1;  $\alpha$  labels type of process.

where  $\sim 0$  implies zero to order  $N$ . The growth is determined by a dynamic balance between these processes and, furthermore, examining the conditions by which Eq. (12) is satisfied provides us with a means of determining the exponent  $\tau$ .

Since the fraction of surface unoccupied by droplets is  $(1 - C)$ , the probability that a new droplet will land on the surface and not coalesce will also scale like  $(1 - C)$ , that is, like  $N$ , and so  $\dot{n}_1 \sim N$ . Because the change in surface coverage due to such a process is just the footprint for an isolated droplet,  $\dot{c}_1 \sim N$ . The  $\alpha = 1$  case satisfies Eq. (12) trivially therefore.

The 2(a) case is less trivial. The probability that a new droplet impinges on an island of radius  $r$  scales as  $r^d$ . The resulting increase in area is  $r^{d-1}dr$ , where the increment in radius is  $dr \sim r^{-(D-1)}$ . As a result  $\dot{c}_{2a} \sim M_{(2d-D)/D}$ . If this is to scale like  $N$ , Eq. (6) imposes the condition  $\tau \geq 2d/D$ .

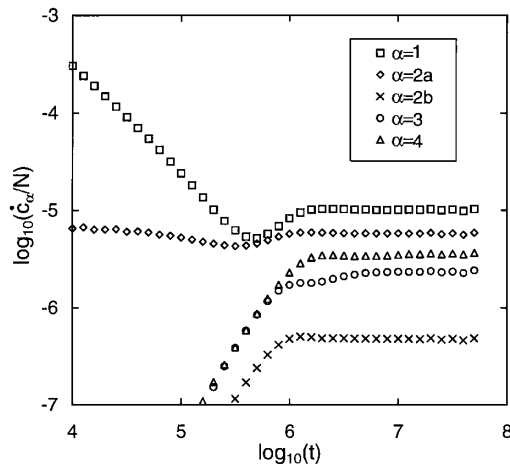


FIG. 3. Plots of  $\dot{c}_\alpha/N$  against time for same system as Fig. 1;  $\alpha$  labels type of process. For clarity, the plots for 1 and 2(a) have been shifted upward by 0.5 and 0.25, respectively.

For case 2(b), we need to evaluate the probability that a droplet lands on an island of radius  $r_i$ , which then expands and overlaps a second island of radius  $r_j$ . The probability for  $d = 2$  and  $D = 3$  is proportional to  $(r_i + r_j)N_iN_j/N$ . A straightforward generalization to arbitrary dimensions yields

$$\dot{n}_{2b} \sim N^{-1} \sum_{i,j} (i^{1/D} + j^{1/D})^{(d-1)} \times (i^{(d+1-D)/D} + j^{(d+1-D)/D})N_iN_j. \quad (15)$$

An expression similar (but without the  $N^{-1}$  prefactor) to Eq. (15) for the  $d = 2$  case has appeared in earlier work [17,22,23]. The expression used in previous work is correct for the early stages of growth. However, in the coalescence regime, droplets are tightly packed with the characteristic length scale,  $2r_0$ , determining their closeness. We have to use the probability ( $\sim N_j/N$ ) that an adjacent droplet has radius  $r_j$ , rather than, as in the early stages of growth, the probability ( $\sim N_j$ ) that the droplet is there at all. The expression for  $\dot{c}_{2b}$  is similar to Eq. (15), but with an extra factor  $i^{d/D} + j^{d/D} - (i^{d/D} + j^{d/D})$  within the summation.

Using the scaling forms from Eqs. (1) and (2), one can show that time evolution of  $\dot{n}_{2b}$  scales as  $t^{z(\tau-\theta)}$  or  $t^{z(2d/D+1-\tau-\theta)}$  according, respectively, to whether small or large sizes are more important in the double summation in Eq. (15). For the first to dominate so that  $\dot{n}_{2b} \sim N$ , we require that  $\tau \geq d/D + \frac{1}{2}$ . A similar consideration of  $\dot{c}_{2b}$  leads to the condition  $\tau \geq 3d/2D + \frac{1}{2}$ .

The probability that an impinging droplet bridges a pair of islands of radii  $r_i$  and  $r_j$  is needed for case 3. For  $d = 2$  and  $D = 3$ , this probability is proportional to  $[r_i r_j (r_i + r_j)]^{1/2} N_i N_j / N$ , which can be generalized to

$$\dot{n}_3 \sim N^{-1} \sum_{i,j} [i^{1/D} j^{1/D} (i^{1/D} + j^{1/D})]^{(d-1)/2} N_i N_j. \quad (16)$$

For  $\dot{c}_3$ , the extra factor is included in the summation as for the previous case.

Following a similar procedure to case 2(b), the conditions we need to satisfy if  $\dot{n}_3$  and  $\dot{c}_3$  are to scale like  $N$  are, respectively,  $\tau \geq 3(d-1)/4D + 1$  and  $\tau \geq (5d-3)/4D + 1$ .

The conditions that dominate are  $\tau \geq 3d/2D + \frac{1}{2}$  if  $D \leq D_c$ , and  $\tau \geq (5d-3)/4D + 1$  if  $D \geq D_c$ , where  $D_c = (d+3)/2$ . Examination of the case 4 cascade effects shows that their incipient processes [2(b) or 3] dominate their time dependences. The conditions just noted will also ensure that case 4 processes scale with  $N$ .

We consider the two limits  $D \rightarrow \infty$  and  $D \rightarrow d$  where, respectively,  $\theta \rightarrow 1$  and  $\theta \rightarrow 2$ . The two expressions for  $\tau$  are consistent with the condition  $\theta \geq \tau$  in these limits only if the equality rather than the inequality is used. We assume that the equality applies throughout the range of

TABLE I. Comparison of  $\tau$  and  $z'$  from Eqs. (17) and (18) with results from Family and Meakin (FM) simulations [8]. There appears to be a typographical error in Table I of [8]. Values (\*) are from Figs. 10 and 11 of Ref. [8].

$d$	$D$	$z$ (FM)	$z$	$\tau$ (FM)	$\tau$	$z'$ (FM)	$z'$
1	1.5	2.94	3.00	1.48	1.50	0.51	0.50
1	2	1.97	2.00	1.25*	1.25	0.49*	0.50
1	3	1.47	1.50	1.18	1.17	0.27	0.25
1	4	1.28	1.33	~1.25	1.13	0.18	0.17
1	8	1.10	1.14	~1.12	1.06	0.079	0.071
2	3	2.92	3.00	1.54	1.58	0.26	0.25
2	4	1.84	2.00	1.45	1.44	0.195	0.125
2	8	1.26	1.33	~1.25	1.22	0.083	0.042

dimensions leading to the final result,

$$\begin{aligned}\tau &= \frac{3d}{2D} + \frac{1}{2}, \quad \text{if } D \leq D_c, \\ &= \frac{5d-3}{4D} + 1, \quad \text{if } D \geq D_c.\end{aligned}\quad (17)$$

The corresponding expressions for  $z'$  are

$$\begin{aligned}z' &= \frac{1}{2}, \quad \text{if } D \leq D_c, \\ &= \frac{3-d}{4(D-d)}, \quad \text{if } D \geq D_c.\end{aligned}\quad (18)$$

A selection from the computer simulation results of Family and Meakin [8] is listed in Table I. For  $d = 1$ , the agreement is excellent for all  $D$ . In particular, the predicted value  $z' = \frac{1}{2}$  is reproduced for  $D \leq D_c$  ( $D_c = 2$  for  $d = 1$ ).

For  $d = 2$ , the  $D = 3$  case is perhaps of most interest. The agreement for both  $\tau$  and  $z'$  is again excellent. At higher values of  $D$ , the agreement between simulations and the current theory remains very reasonable for  $\tau$ , but deteriorates for  $z'$ . The reason for this is the excessive time required in the simulations to reach the asymptotic limit where the scaling relations apply exactly. The degree to which Eqs. (8) and (9) are satisfied is a measure of how closely a simulation has approached the scaling regime.

For one and two dimensional substrates, the current theory gives an excellent account of the polydispersity behavior, and any discrepancies with the results from simulations can be fully accounted for by the difficulty for simulation in attaining the asymptotic regime.

We conclude with some comments on three dimensional substrates. For this case,  $D_c = 3$  and, since  $D > d$ ,  $\tau = 1 + 3/D$  and  $z' = 0$ . Hence  $\tau = \theta$  for all values of  $D$ . Simulations [8] are unable to distinguish  $\tau$  and  $\theta$ , and report very small values of  $z'$ . Within the limitations of simulations, already noted, there is consistency with the

present theory. An exponent of zero deduced from scaling theory usually implies logarithmic terms. Since the theory yields a value of  $z'$  of zero, we infer that  $N$  approaches zero logarithmically. In turn this implies that  $d = 3$  is the upper critical dimensionality for the droplet growth process. We have also done simulations for  $d = 4$ ,  $D = 5$  and found that  $z$  is in the range 4.6–4.8 which is, within error limits, in agreement with the prediction of 5 from Eq. (8). The basic scaling hypothesis is still applicable therefore, but the details of the polydispersity will be different for  $d > 3$ . We will report on these matters more fully elsewhere, together with a more detailed study of the  $d = 1$  and  $d = 2$  cases.

This work was performed when one of us (S. B.) was a Visiting Scientist at the University of Reading.

- 
- [1] P. Meakin, Rep. Prog. Phys. **55**, 157 (1992).
  - [2] D. Beysens and C.M. Knobler, Phys. Rev. Lett. **57**, 1433 (1986).
  - [3] J.L. Viovy, D. Beysens, and C.M. Knobler, Phys. Rev. A **37**, 4965 (1988).
  - [4] H. Zhao and D. Beysens, Langmuir **11**, 627 (1995).
  - [5] D. Beysens, Atmos. Res. **39**, 215 (1995).
  - [6] E. Grantscharova and D. Dobrev, Thin Solid Films **161**, 213 (1988).
  - [7] F. Family and P. Meakin, Phys. Rev. Lett. **61**, 428 (1988).
  - [8] F. Family and P. Meakin, Phys. Rev. A **40**, 3836 (1989).
  - [9] M. Zinke-Allmann, L.C. Feldman, and W. van Saarloos, Phys. Rev. Lett. **68**, 2358 (1992).
  - [10] G.R. Carlow, R.J. Barel, and M. Zinke-Allmann, Phys. Rev. B **56**, 12 519 (1997).
  - [11] M. Zinke-Allmann, Thin Solid Films **346**, 1 (1999).
  - [12] L. Haderbache, R. Garrigos, R. Kofman, E. Søndergård, and P. Cheyssac, Surf. Sci. **410**, L748 (1998).
  - [13] E. Søndergård, R. Kofman, P. Cheyssac, and A. Stella, Surf. Sci. **364**, 467 (1996).
  - [14] T. Aste, R. Botter, and D. Beruto, Sens. Actuators B, Chem. **24–25**, 826 (1995).
  - [15] H. Lannibois, A. Hasmy, R. Botet, O.A. Chariol, and B. Cabane, J. Phys. (Paris) II **7**, 319 (1997).
  - [16] S.-G. Kang, A. R. Kerstein, J.J. Helble, and A. F. Sarofim, Aerosol Sci. Technol. **13**, 401 (1990).
  - [17] R. Vincent, Proc. R. Soc. London A **321**, 53 (1971).
  - [18] B. Derrida, C. Godreche, and I. Yekutieli, Europhys. Lett. **12**, 385 (1990).
  - [19] K. Pesz and G.J. Rodgers, J. Phys. A **25**, 705 (1992).
  - [20] B. Briscoe and K. Galvin, Phys. Rev. A **43**, 1906 (1991).
  - [21] A. V. Osipov, Thin Solid Films **261**, 173 (1995).
  - [22] J. A. Blackman, Physica (Amsterdam) **220A**, 85 (1995).
  - [23] S. Cueille and C. Sire, Phys. Rev. E **57**, 881 (1998).
  - [24] N. V. Brilliantov, Y.A. Andrienko, P.L. Krapivsky, and J. Kurths, Phys. Rev. E **58**, 3530 (1998).
  - [25] T. Aste, Phys. Rev. E **53**, 2571 (1996).
  - [26] N. Standish, A. B. Yu, and R. P. Zou, Powder Technol. **68**, 175 (1991).